

On-chip acoustophoretic isolation of microflora including *S. typhimurium* from raw chicken, beef and blood samples

Bongkot Ngamsom,¹ Maria J. Lopez-Martinez,¹ Jean-Claude Raymond,² Patrick Broyer,³ Pradip Patel,² and Nicole Pamme^{1,a)}

¹Department of Chemistry, University of Hull, Hull, HU6 7RX, UK

²bioMérieux Innovation, Chemin de l'Orme, Marcy l'Etoile, 69280, France

³bioMérieux Innovation /Technology Research Lab, Grenoble, 38024, France

Pathogen analysis in food samples routinely involves lengthy growth-based pre-enrichment and selective enrichment of food matrices to increase the ratio of pathogen to background flora. Similarly, for blood culture analysis, pathogens must be isolated and enriched from large excess of blood cells to allow further analysis. Conventional techniques of centrifugation and filtration are cumbersome, suffer from low sample throughput, are not readily amenable to automation and carry a risk of damaging biological samples. We report on-chip acoustophoresis as a pre-analytical technique for the resolution of total microbial flora from food and blood samples. The resulting 'clarified' sample is expected to increase the performance of downstream systems for the specific detection of the pathogens. A microfluidic chip with three inlets, a central separation channel and three outlets was utilized. Samples were introduced through the side inlets, buffer through the central inlet. Upon ultrasound actuation, large debris particles (10-100 μm) from meat samples were continuously partitioned into the central buffer channel, leaving the "clarified" outer sample streams containing both, the pathogenic cells and the background flora (ca. 1 μm) to be collected over a 30 min operation cycle before further analysis. The system was successfully tested with *Salmonella typhimurium*-spiked (ca. 10^3 CFU mL^{-1}) samples of chicken and minced beef, demonstrating a high level of the pathogen recovery (60-90%). When applied to *S. typhimurium* contaminated blood samples (10^7 CFU mL^{-1}), acoustophoresis resulted in a high depletion of the red blood cells (99.8%) which

partitioned in the buffer stream, whilst sufficient numbers of the viable *S. typhimurium* remained in the outer channels for further analysis. These results indicate that the technology may provide a generic approach for pre-analytical sample preparation prior to integrated and automated downstream detection of bacterial pathogens.

1. Introduction

Foodborne diseases have long been a threat to public health and safety. A total of 19,531 infections, 4,563 hospitalizations and 68 deaths associated with foodborne diseases, e.g. *Salmonella*, *Escherichia coli* 0157:H7, *Listeria*, *Campylobacter*, were reported in 2012 in the US by The Foodborne Diseases Active Surveillance Network (FoodNet).¹

Conventional steps in the analysis of pathogens in food comprise of (i) cultural pre-enrichment of samples to allow the resuscitation and growth of the pathogen, as well as the associated intrinsic flora; (ii) cultural selective enrichment to inhibit the growth of the background flora, resulting in a high pathogen ‘signal-to-noise’ ratio; (iii) selective plating to allow the growth of the specific pathogen, whilst restricting or inhibiting the background flora; and (iv) the pathogen, if present, is presumptively detected as a ‘typical’ colored colony on a selective plate, and further identified by biochemical, immunological, serological and genetic tests. The process is cumbersome, and time- and labor-intensive, e.g. *Salmonella* analysis can take from 3-5 days.² Numerous more rapid detection systems, including those based on immunology (e.g. Vidas from bioMérieux³) and molecular biology (e.g. BaxTM from DuPont⁴) are now available that can reduce the analysis time to 24-48 h, depending on the types of pathogen and the matrix under investigation.

Due to the modern global food supply chain and the regulatory pressures to increase the safety of food for the ‘knowledgeable’ consumer, there is a greater need to provide analytical results even quicker. Several non-culture approaches, based on capture and concentration of the target pathogen from complex samples prior to detection, have been reported for this

purpose, including immunomagnetic and phage protein coated micro- and nano-magnetic beads.⁵⁻⁸ These techniques allow quicker and robust detection of the pathogen from certain matrices due to reduction of the background interferences (e.g. PCR inhibitors for molecular detection), as well as the concentration of the pathogen. However, they also have limitations, particularly the loss of beads due to fatty components in matrices and the relatively high cost of the beads.⁹⁻¹¹ Whilst efforts have been made to speed up sample analysis, the pre-processing remains a bottleneck, particularly in terms of its performance and ease with which it can readily integrate cost-effectively within the normal customer analytical workflows which increasingly rely on downstream automated detection platforms.

For clinical analysis, conventional macroscale separation processes based on centrifugation, filtration, chromatography and electrophoresis have commonly been employed for many decades. However, such methods suffer from time-consuming steps, very low throughput or risks of damaging biological samples.^{2, 12, 13}

Continuous flow separation methods in microfluidic devices may address the challenge of sample preparation as they allow processing in continuous flow which is amenable to automating and integration with downstream analysis steps.^{5, 9, 10} A number of different forces have been successfully utilized for continuous flow sorting of cells and particles on-chip,^{12, 14} including inertia electrokinetic,^{15, 16} dielectrophoretic,¹⁷⁻¹⁹ magnetophoretic²⁰ and mechanical contact forces. Acoustophoresis is a particularly interesting technique in this context, as it allows gentle and label-free separation of micrometer sized particles and cells based on their size, density and compressibility compared to the surrounding medium.^{14, 21-33}

The principle of acoustophoresis is based on a radiation force (F_r) that is exerted upon suspended particles in the presence of a resonant acoustic field.³² The radiation force (equation 1) is a function of the wavelength (λ) of the acoustic standing wave, the applied pressure

amplitude (p_0), the particle volume (V_p), the particle density (ρ_p) and compressibility (β_p) as well as the medium density (ρ_m) and compressibility (β_m):

$$F_r = - \left(\frac{\pi V_p \beta_m p_0^2}{2\lambda} \right) \phi(\beta, \rho) \sin\left(\frac{4\pi x}{\lambda}\right) \quad (1)$$

with $\phi(\beta, \rho) = ((5\rho_p - 2\rho_m)/(2\rho_p - 2\rho_m)) - (\beta_p/\beta_m)$ as the acoustic contrast factor. Particles will be moved towards the pressure node if the contrast factor is positive ($\phi > 0$), and to the pressure anti-node for negative value ($\phi < 0$). For example, erythrocytes ($\phi \approx 0.3$) should move towards a pressure node whilst triglycerides ($\phi \approx -0.3$) move towards the pressure anti-node.²²

The radiation force, exerted mainly on larger size particles ($> 2 \mu\text{m}$), is directly proportional to the particle volume (V_p) and, therefore r^3 . Thus, a slight difference in the particle size will significantly affect the radiation force. This effect has been used to sort particles from suspensions or from biological fluids.³¹ Most studies have reported the acoustic focussing of particles or cells of interest into the pressure nodes to isolate them from the original samples.^{14, 21-33}

Another force created by a standing ultrasonic wave in a microchannel containing a microparticle suspension is the Stroke drag force from the induced acoustic streaming flow.^{34, 35} The acoustic streaming mostly affects particles $< 2 \mu\text{m}$. An investigation of the lateral motion of yeast cells and polymer beads (1 to 25 μm) in a half wavelength standing wave device with an acoustic frequency of ca. 3 MHz showed that the larger particles ($> 10 \mu\text{m}$) focused into the center of the pressure nodal plane, whilst the 1 μm particles did not as the drag from acoustic streaming dominated the lateral radiation force.³⁴

The current investigation focuses on resolving undesired large particles ($\sim 10 - 100 \mu\text{m}$) from the intrinsic microflora (or spiked *S. typhimurium*) ($\sim 1 \mu\text{m}$ in size) present in complex sample matrices by acoustophoresis. This is needed because of a number of reasons: (i) direct filtration ($> 0.45 \mu\text{m}$ filters) of complex food matrices is not possible due to clogging of the

filters, whilst high speed centrifugation will concentrate both the microflora as well as the intrinsic particulates; and (ii) the presence of large particulates containing the target pathogen can interfere with the subsequent downstream detection (e. g. flow cytometry and q-PCR).³⁶⁻³⁸

To achieve this, the fluid containing food particulates or blood enters the microfluidic device via the side inlets in parallel with the medium/buffer in the central channel in a laminar flow regime (Fig. 1). An ultrasonic standing wave with a pressure node in the center of the channel is established via a piezoceramic transducer (Pz). The resulting acoustic radiation forces on the sample components drives the larger particles such as pieces of debris or red blood cells (ca. 8 μm) into the central buffer stream. In contrast, the microbial cells, which experience significantly less acoustic radiation force, continue flowing through the separation channels and are collected as ‘clarified’ samples at the exits for further downstream analysis.

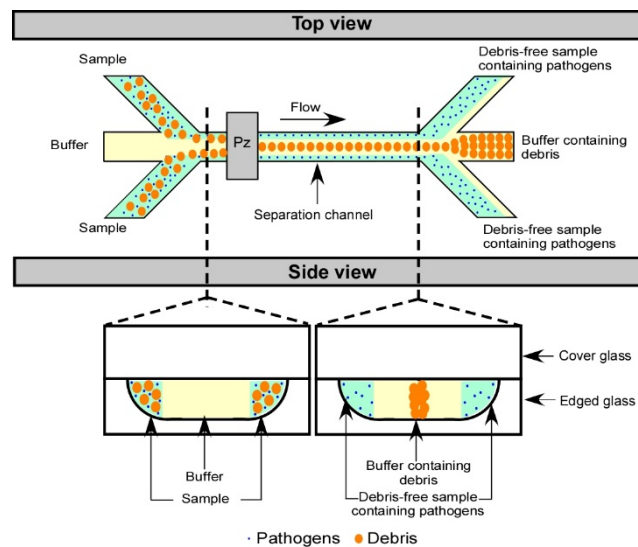


Fig. 1. Resolution of large food debris particles or red blood cells from smaller intrinsic microflora or spiked *S. typhimurium* by acoustophoresis under ultrasonic radiation force. Debris particles focus at the pressure nodal plane in the central outlet containing the buffer stream, whilst the microbial cells remain in the sample streams exiting the side outlets.

2. Materials and methods

2.1. Microfabrication

The chip design featured three inlets, a single 30 mm long central channel for focussing and three outlet channels (Fig. 2a). Inlet and outlet channels were drawn at a 45° angle.³² The chip was fabricated in glass in-house (University of Hull, UK).³⁹ Briefly, the design was patterned onto 1 mm glass wafers coated with a chromium layer and photoresist layer. After development, the glass was etched with hydrofluoric acid (HF) yielding microchannels with a depth of 100 μm , 305 μm width at the bottom and 590 μm width at the top. Access holes were drilled into the etched glass slide before it was thermally bonded to a cover plate to achieve a closed structure.

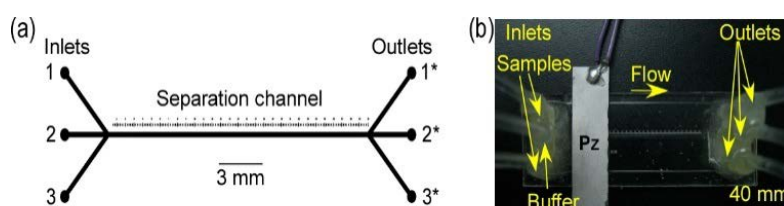


Fig. 2. (a) Design of the microfluidic chip featuring a 30 mm long, 100 μm deep and 590 μm wide separation channel, three inlet and three outlet channels. (b) Photograph of the microfluidic device, with the piezoelectric transducer attached to the top.

2.2. Acoustophoresis set-up

The piezoceramic element (Pz26, Ferroperm Piezoceramics, Denmark) was attached to the top side of the microfluidic chip by ultrasound gel (Anagel, TM UK), Figure 2b. The chip holes were connected to the sample delivering/collecting three syringes via tailored micropipette tips (Eppendorf, UK) and Tygon tubing (0.762 mm ID, 2.286 mm OD, Cole-Parmer, UK). Three syringe pumps (Harvard Apparatus, UK) equipped with 5 mL plastic syringes (BD Plastipak) were used to control the flow rates at the inlets and the outlets. One

pump with two syringes was used to deliver the sample (polystyrene particles or unspiked/*S. typhimurium*-spiked chicken, beef and blood) to the two side inlet channels of the microfluidic chip. The second pump with two syringes was used to control flow of the buffer medium into the central channel. The third pump was connected to the three outlet channels, via three syringes, to achieve a stable flow profile. For polystyrene particle and food samples, the inlet flow rates for sample and buffer were 10 and 30 $\mu\text{L min}^{-1}$, respectively. For blood, the sample and the buffer flow rates were 10 and 70 $\mu\text{L min}^{-1}$, respectively. At each outlet, fluid was withdrawn at 1/3 of the total inlet flow rate, i.e. 16.67 $\mu\text{L min}^{-1}$ and 30 $\mu\text{L min}^{-1}$ for the food (& polystyrene) samples and blood, respectively.

The acoustic standing wave was generated by applying an alternating current (AC) signal fed into the circuit by a function generator (Agilent, Model 33210A, 10 MHz function/arbitrary waveform generator, UK) operating at its sinusoidal mode. An amplifier (Amplifier research, Model 1W1000B, 1-1000 MHz, AR) was employed to amplify the signal from the function generator to obtain the required voltages. An oscilloscope (Tektronix, Model TBS 1042, USA) was connected in parallel to the transducer to measure the operating voltage. To achieve a single nodal plane in the microfluidic channel, the ultrasonic waves were actuated at 1.303 MHz, 37.4 Vp-p for the experiments involving polystyrene beads and food samples. For the blood experiments, the settings were 1.300 MHz and 37.0 Vp-p. Flow in the microfluidic chip was observed through an inverted microscope (Nikon Eclipse Ti, UK) with 4x objective lens, equipped with a high resolution CCD camera (Retiga EXL, Canada) for imaging. The behaviour of the particles within the channels was monitored by InterVideo Win DVD software.

2.3. Characterization of acoustophoretic resolution by spectrometry and particle size distribution

The extent of acoustophoretic resolution of chicken food particles from the intrinsic natural microflora (and spiked *S. typhimurium*) was determined by measuring the optical density (600 nm; UV-Vis Spectrophotometer; UV Mini 1240, Shimadzu Scientific, USA) before and after acoustophoresis of the samples. The particle size distribution of food samples were determined by Photon correlation spectroscopy (PCS) using a Mastersizer 2000 (Malvern Instrument Ltd, UK). The side outlet samples (ca. 5 mL) from the microfluidic chip operated with and without ultrasound were diluted with BPW (ca. 100 mL) at the dispersion unit controller at 1500 rpm before analysis using a laser intensity of 87.4%.

2.4. Cultural plating

The level of microflora in food samples was determined off-chip by cultural plating. Total viable count (TVC) of food samples was estimated according to ISO 7218⁴⁰ by enumerating the number of colonies on Trypticase Soy Agar (TSA) after incubation at 37 °C for 48 h. The number of presumptive *S. typhimurium* colonies was determined by plating appropriate sample dilutions on the selective chromID®-Salmonella medium (bioMérieux, France).

2.5. Polystyrene beads

For initial acoustophoresis process characterization and optimization, a 10 v% suspension of 30 µm polystyrene beads (Polysciences, Inc., USA) in phosphate buffered saline (PBS) solution containing 0.05% Tween 20 was prepared.

2.6. *S. typhimurium* control inoculum

An isolated colony of *S. typhimurium* (NCTC 12023/ATCC® 14028, Pro-lab Diagnostics, UK) on TSA was diluted in 9 mL tryptic soy broth (TSB) and incubated at 37 °C for 18 h. A portion (0.2 mL) of the broth was diluted in 9 mL BPW and its absorbance was measured at 600 nm (CECIL 1011 spectrometer, 1000 Series) to obtain a reading of 0.070

absorbance units (corresponding to ca. 1.5×10^8 CFU mL⁻¹). To confirm the actual level in the broth, a series of decimal dilutions were prepared (d-1 to d-5 corresponding to ca. 10^7 to 10^3 CFU mL⁻¹). Then 100 µL of d-5 was plated on TSA and incubated overnight at 37°C. This process was carried out in duplicate. The level of *S. typhimurium* present was calculated by counting the number of colonies on the plate and taking account of the dilution factor. An appropriate dilution was used to spike the food samples.

2.7. Unspiked food samples

Chicken portions (wings with skin, legs with skin, breasts with and without skin as well as neck with skin) and minced beef samples were purchased from three local supermarkets (Morrisons, Tesco and Asda). The samples were used within the same day. The meat was cut with a sterile scalpel. Samples (10 g) were placed inside separate filter bags (TEMPO BAG, bioMérieux, France) and each mixed with 90 mL buffered peptone water (BPW; bioMérieux, France), before homogenization for 30 s in a Stomacher (IUL Instruments, Germany). The prepared samples were incubated at 37 °C for 3 h. A volume (10 mL) from each sample was taken from the membrane side of the filter bag and used directly for the acoustophoretic analysis.

2.8. *S. typhimurium*-spiked food samples

Portions (10 g) of each sample were placed inside separate filter bags and each mixed with 90 mL BPW before homogenization as described previously. Without further incubation, for each of the sample, a volume (10 mL) was taken from the membrane side of the filter bag and spiked with 0.1 mL of *S. typhimurium* (ca. 10^5 CFU mL⁻¹) to give a final concentration of ca. 10^3 CFU mL⁻¹. Each sample was used directly for the acoustophoretic analysis.

2.9. *S. typhimurium*-spiked and unspiked blood samples

Defibrinated horse blood (9 mL; Oxoid, ThermoScientific, UK) was filtered through a 100 µm filter (Porex Corporation, USA) and mixed with 1 mL of 3.2 % (w/v) trisodium citrate to prevent the blood clotting. The mixture was then diluted in PBS solution (1:1 volume ratio)

and spiked with ca. 10^7 CFU mL⁻¹ *S. typhimurium*. Both, spiked and unspiked samples were subjected to acoustophoresis. The extent of depletion of red blood cells (RBCs) from the blood subjected to acoustic actuation was measured by a haemocytometer. The percentage depletion was calculated from the number of RBCs emerging from the central outlet as a function of the total number of RBCs emerging from all the outlets and expressed as a percentage.

3. Results

3.1. Separator design and performance

The chip used was based on a design reported previously³² featuring three inlets, a single separation channel and three outlets. The channel width corresponds to half the wavelength of the ultrasonic standing wave. However, unlike the previous design (375 μ m width, 2 MHz frequency), the present study used a wider channel (590 μ m) to minimize the risk of any blockage with the food samples that can contain debris of varying particulate sizes. The wider channel was expected to lead to a lower operating frequency (ca. 1.3 MHz) and, thus, to reduced acoustic forces by about 40% as per Equation 1. The functionality of the wider channel was initially verified with 30 μ m polystyrene beads sample applied to the inlets 1 and 3 at 10 μ L min⁻¹, whilst PBS buffer was pumped into the inlet 2 at 30 μ L min⁻¹ (Fig. 3a). Without ultrasonic actuation, the particles will follow laminar flow pattern, the particles will be pushed near to the separation channel walls and exit at the side outlets (1* and 3*), whilst the clear buffer solution exit through the central outlet (2*); results not shown in this figure. Upon acoustic actuation, the beads migrated from the separation channel walls and focussed as a narrow band at the pressure nodal band located in the buffer stream at the centre of the separation channel (Fig. 3b). By visual inspection and video recording, the best focussing was found to occur at an operating frequency of 1.303 MHz; the beads focussed at ca. 2 cm from the start of the separation channel ($F_r \approx 7.8$ nN). This set-up was tested with the food and blood samples.

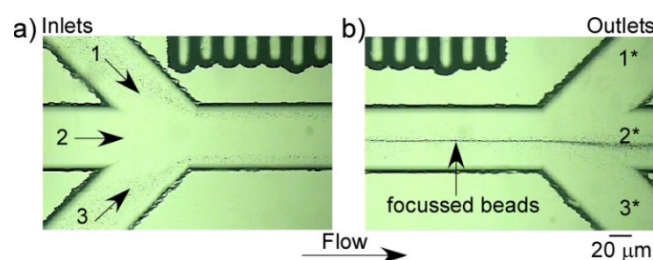


Fig. 3. Microscope photographs showing (a) the inlets and part of the separation channel, and (b) the outlets and part of the separation channel. The polystyrene beads entered the separation channel via the side inlets (1 and 3) and located in the outer part of the separation channel under the laminar flow regime (a). Upon ultrasonic actuation, the beads were acoustically focussed at the pressure node at the centre of the separation channel and exited the central outlet (b).

3.2 Acoustophoresis of food broths

The microfluidic device was tested with a range of heterogeneous chicken and beef homogenates to assess their acoustic focussing characteristics. Without acoustic actuation (referred to as “OFF”), the food sample flowed along the outer part of the separation channel and exited via the side outlets (1* and 3*) as expected from the laminar flow regime (Figure 4b). Upon actuation (referred to as “ON”), the majority of the food particles were focussed into the central buffer stream and exited through the central “waste” outlet (2*) (Fig. 4a/b). Fig. 4b shows that the acoustic focussing of chicken particulates into the central outlet results in an optically “clearer” sample exiting the side outlets.

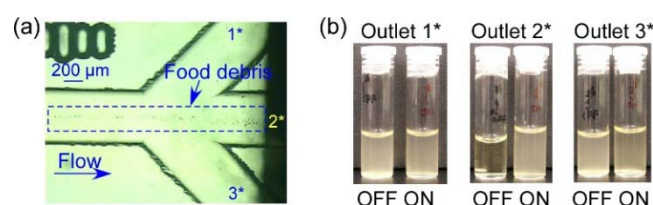


Fig. 4. (a) Focussing of particulates from a chicken sample into the central outlet (2*) of the microfluidic chip upon acoustic actuation. (b) Photographs showing samples collected from the chip outlets with (‘ON’) and without (‘OFF’) ultrasonic actuation.

3.3. Characterization of the acoustophoretic resolution of food broths

PCS measurements of the fluids collected from the outlets 1* and 3* are shown in Fig. 5. The spectrum shows a marked reduction in the large particulates (10-100 µm), with concomitant increase in smaller particles (1 µm), in the chicken sample streams subjected to

acoustic actuation. The large particles were driven towards the pressure node in the center of the separation channel. According to Equation 1, a radiation force of approximately 3000x smaller was also exerted on smaller particles. Similar PCS results were observed for all the food samples tested. The optical density (A600nm) of the samples emerging from the side outlets (1* and 3*), with and without acoustic actuation, was also measured (Fig. 6). Except for the chicken neck sample (~25%), the optical densities of all the other food samples tested were reduced on average ~50% (range 43 - 53 %) on application of acoustophoresis.

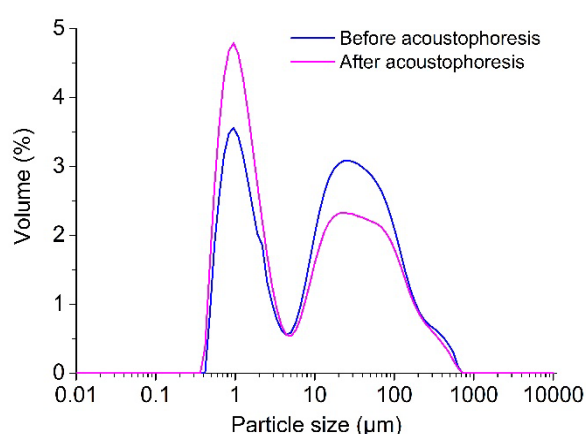


Fig. 5. PCS measurements showing the spectrum of particulates in chicken sample streams emerging from the outlets 1* and 3*, with and without application of acoustophoresis.

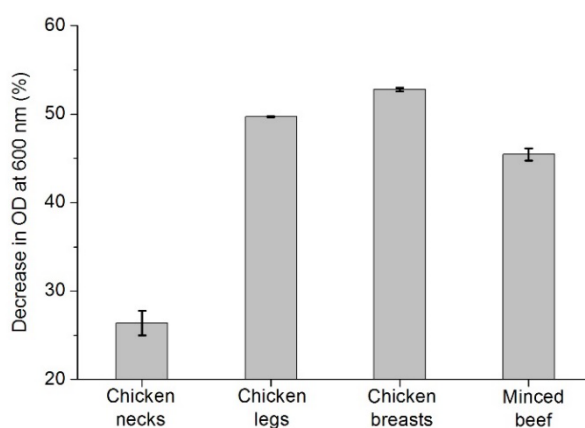


Fig. 6. Decrease in optical density (A600nm) of food samples subjected to acoustophoresis (n=3).

3.4. Acoustophoretic resolution of food particles from intrinsic natural microflora

Fig. 7 shows the effect of acoustophoresis on the levels of TVC in the food streams emerging from the chip outlets (1* and 3*), with/without application of the acoustic radiation. No significant loss of viable microorganisms was observed, although there was a significant reduction in the optical density in the streams emerging from the outlets (1* and 3*) on application of acoustophoresis (Fig. 4 and 6). In the absence of acoustic radiation, TVC (range $10^6 - 10^8$ CFU g⁻¹) was enumerated in the outlets (1* and 3*) as expected, but not in the buffer stream emerging from the central outlet (data not shown), confirming establishment of a laminar flow. In the 'ON' position, an equivalent level of TVC was measured in all the outlet channels, indicating that organisms may be associated with the particles and/or microbial aggregation may lead to larger particle sizes that partition in the central channel. Fig. 7 also shows that the viability (TVC) of organisms is not adversely affected by acoustophoresis. This finding is important for further downstream analysis and, in general, for the microbiological examination of foods. However, it should be noted that the standard colony count method requires ~ 24 h plate incubation, which can allow recovery of any non-lethal transient microbial damage that may have been caused by acoustophoresis.

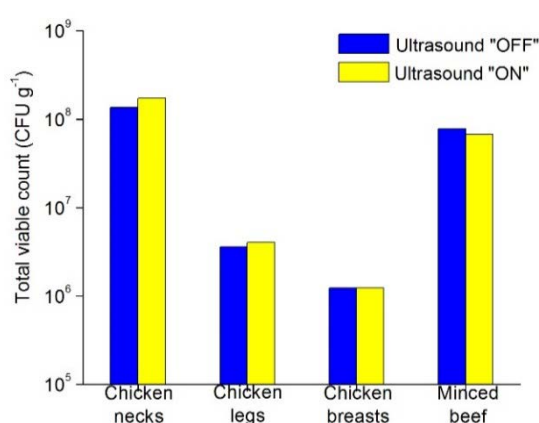


Fig. 7. Level of TVC emerging from the outlets 1* and 3* with (yellow bars) and without (blue bars) ultrasonic radiation.

3.5. Acoustophoretic resolution of food particles from *S. typhimurium*-spiked chicken and beef samples

The aim was to determine if *S. typhimurium* remained in the original food streams on application of the acoustic radiation and exited the outlets 1* and 3*, as observed with the natural microbial flora (Fig. 7). The results are summarized in Fig. 8. Regardless of sample type, presumptive-positive *Salmonella* colonies were enumerated only in the fluid collected from the side outlets (1* and 3*) when the ultrasound was switched off. This confirmed that a laminar flow was correctly established. With ultrasound switched on, a high recovery (60-96%) of *S. typhimurium* was obtained from the side outlets (1* and 3*), whilst ~ 5-10 fold lower numbers were noted in the central outlet (2*). This may be attributed to carry over of some of the *S. typhimurium* cells with the food matrix particulates that cross into the central buffer channel. The level of *Salmonella* recovery in the ‘clarified’ streams existing the outlets (1* and 3*) was considered significant for further downstream concentration, detection and identification of the pathogen.

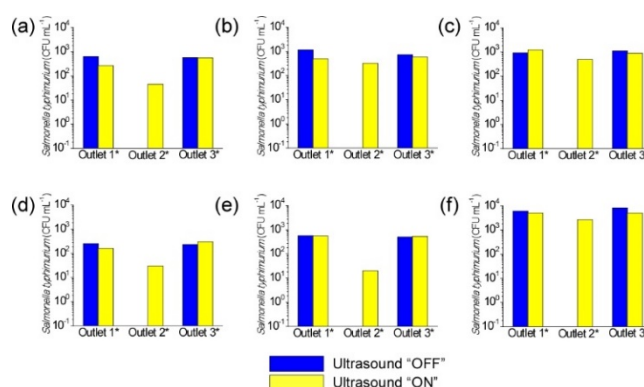


FIG. 8. Level of *S. typhimurium* enumerated in the samples collected from the chip outlets with (yellow bars) and without (blue bars) acoustic actuation. a - c and d - f; three different chicken and mince samples, respectively.

3.6. Acoustophoretic isolation of unspiked and *S. typhimurium*-spiked blood

The chip used for the microbial resolution from food particulates was also applied to the blood matrix to determine if the chip design was generic enough to apply across widely different matrices. Pre-filtration of blood samples using a 100 μm filter was employed in the sample preparation; the process took less than a minute to perform and prevented the chip from clogging. Fig. 9 shows the results for unspiked *S. typhimurium*-spiked blood. Visual observation clearly shows that the RBCs were focused in the central stream (2*) upon acoustic activation. However, on closer examination, it was found that a low percentage (0.2%) of the cells exited the side outlets (1* and 3*). Approximately 99.8% of RBCs crossed into the buffer stream, leaving the clear plasma in the outlets 1* and 3* under acoustic radiation.

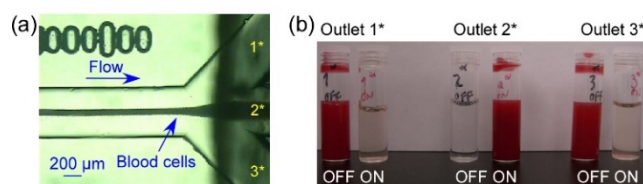


Fig. 9. (a) Effect of ultrasonic actuation on the resolution of RBCs from blood. The RBCs crossed from the outer part of the separation channel and focused into the buffer central stream, leaving the “clear” plasma fraction exiting the outer channels for further analysis; (b) Visual observation of the effect of acoustophoresis (ON) on blood compared with control samples (OFF).

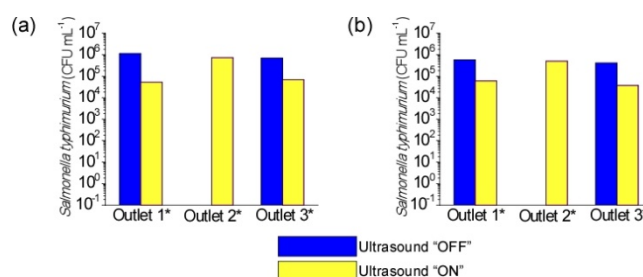


Fig. 10. Level of *S. typhimurium* enumerated in the samples collected from the chip outlets with (yellow bars) and without (blue bars) acoustic actuation. (a) and (b): Two different batches of blood.

4. Discussion

The present study demonstrates the potential of continuous flow acoustophoresis as a rapid and label-free on-chip technology for the resolution of *S. typhimurium* from spiked

food samples. The microfluidic chip for acoustophoresis was designed to have a relatively wide channel (625 μm) to allow large particulates in the food homogenates to flow through without creating blockage problems. For this purpose, a lower frequency (1.3 MHz as opposed to 2 MHz) had to be employed in order to operate at $\lambda/2$ mode, resulting in a lower radiation force (F_r). However, the visual observation and video recording showed that a pressure nodal band located in the centre of the separation channel, where the large particles focussed, was created in all the samples tested regardless of their complexity. The bacterial resolution from the food matrices was highly consistent despite the fact that foods are heterogeneous in nature and their structures create a local physical or chemical environment which affects the spatial distribution of microorganisms.⁴¹

Although the acoustic resolution of low levels (10^2 - 10^3 CFU mL^{-1}) of spiked *S. typhimurium* from the food particulates was not complete, the resulting samples showed a high level of recovery (up to 90%). Potentially, these can be sufficiently ‘clear’ to be of practical value for the subsequent rapid detection of *S. typhimurium* by modern techniques (e.g. immunomagnetic-based qPCR and immunoassays). The combination of acoustophoresis and rapid downstream methods will be assessed in future studies.

Given the highly heterogeneous nature of food homogenates, comprising varying size particulates in colloidal suspensions, it is unexpectedly surprising that the microbial recovery is high. The viability of *S. typhimurium* was not affected by the acoustophoresis process judging from the results obtained by the selective culture procedure. A number of previous reports also showed that acoustophoresis does not affect cell viability and proliferation.^{13,21,33}

The current acoustophoresis chip-based approach for sample ‘decomplexification’, achieved by resolving the intrinsic microflora from complex food particulates, is comparable with microfiltration method reported by Li *et al.* (2013),¹⁰ who showed 70% recovery of *S.*

typhimurium from a chicken sample. Microfiltration based on membranes are prone to fouling from complex heterogeneous samples and, generally, cannot be re-used, whereas clogging in glass chips, if encountered, could be prevented by designing chips with different channel dimensions. The sample volume throughput of the chips can also be increased from the current 2 mL h⁻¹ to larger volumes (e.g. 10 ml) by running the sample through several parallel channels.⁴² This chip format is expected to increase the overall recovery of the pathogen for subsequent rapid analysis.

In clinical diagnostics and infectious disease monitoring, generally, only the RBC-free fraction of the whole blood is used. The conventional processes to extract plasma from the whole blood are centrifugation and filtration, both of which are easy to conduct but have some limitations including low resolution of the RBCs, limitation in the volume throughput, and lack of automation.^{43, 44} An alternative is to assess the potential of the microfluidic acoustophoresis device for this purpose.

The results from acoustophoretic isolation of defibrinated horse blood samples correlate well with the recent findings by Ohlsson *et al.* (2013) where a 99.94 % depletion of blood cells were reported.⁴⁵ In their work, a silicon chip with anisotropically etched channels sealed with a glass lid was employed and the experiment was performed on a Peltier element to allow temperature to be controlled at 25°C. The flow rate of the blood stream was ten-folds higher than that of the present experiment (20 µL min⁻¹), was controlled by a pressure terminal with feedback from flow sensors to compensate flow pulsations. The blood was much more diluted (1%) as opposed to our study (45%). Clearly, the recovery of *S. typhimurium* in the plasma fraction was low (~10%), compared with the high recoveries (60 - 96%) found with different chicken and beef matrices. This difference may be attributed to the adsorption/specific binding (e.g. lectin/glycoprotein interactions)⁴⁶ of *S. typhimurium* to the RBCs partitioned in the nodal band of the central channel. A number of

approaches may be used to improve the recovery, including: adding reagents (saccharides, oligosaccharides or non-toxic levels of surfactants)⁴⁷ to reduce microbial cell adsorption; changing the density of the medium to separate particles with similar sizes;²³ better control of the chip temperature and flow rates;⁴⁵ and higher dilution of the blood sample which can result in higher numbers of the blood cells focussing in the center of the separation channel with less entrapped microbial cells.⁴⁵ Despite the low recovery of *S. typhimurium*, there were still sufficient number of cells in the 'clear' plasma fraction that would allow further downstream analyses (e.g. IMS-based qPCR and flow cytometry). Both, IMS and flow cytometry are known to have practical limitations when used for pathogen detection in complex samples, thus, IMS exhibits reduced pathogen recovery from fatty and particulate samples,⁴⁸ whilst food particles and background fluorescence can interfere in flow cytometry.³⁷ The classical centrifugation technique works well for the separation of plasma from whole blood but it can be tedious, time-consuming, and cannot be easily automated and integrated with downstream analysis. For microbial separation from whole blood, a more cumbersome density gradient centrifugation may well need to be used.

Overall, the microfluidic acoustophoresis technology has a number of key advantages compared with the existing sample preparation processes for the resolution of microbial flora from complex matrices, including ease of automation, low-cost of the chip consumables and generic applicability to varying types of sample matrices.

5. Conclusions

To the authors' knowledge, this is the first time continuous flow microfluidic acoustophoresis chips have been used successfully to demonstrate reproducible resolution of the natural microflora (and spiked *S. typhimurium*) from raw food broths (different portions of chicken and ground beef). In this study, the conventional lengthy non-selective and selective cultural plating techniques were merely used to characterize the extent of resolution of the

intrinsic or spiked microbial flora from the matrices. The extent of recovery of the natural microflora and *S. typhimurium* from the starting turbid and highly particulate matrices into ‘clarified’ sample streams by acoustophoresis is considered of value for future downstream analyses by rapid methods (e.g. IMS-based qPCR and flow cytometry).

Acknowledgements

BN and NP would like to thank C. Murphy for her kind support on biological sample preparation and analyses. Microfluidic chip fabrication by S. Clark is also gratefully acknowledged. Our sincere gratitude is expressed to Dr M.D. Tarn for all helpful input to the manuscript. The work was financially supported by bioMérieux s.a., Chemin de l’Orme, Marcy l’Etoile, 69280, France.

References

1. D. Gilliss, M. Cartter, M. Tobin-D’Angelo, D. Blythe, K. Smith, S. Lathrop, S. Zansky, P. R. Cieslak, J. Dunn, K. G. Holt, S. M. Crim, O. L. Henao, M. Patrick, P. M. Griffin and R. V. Tauxe, *MMWR* **62** (15), 283-287 (2013).
2. P. Patel, *J Rapid Meth Aut Mic* **8** (4), 227-248 (2000).
3. V. Jasson, L. Baert and M. Uyttendaele, *Int J Food Microbiol* **145** (2-3), 488-491 (2011).
4. S. R. Nugen and A. J. Baeumner, *Anal Bioanal Chem* **391** (2), 451-454 (2008).
5. H. Wang, Y. B. Li, A. Wang and M. Slavik, *J Food Protect* **74** (12), 2039-2047 (2011).
6. M. Varshney, L. J. Yang, X. L. Su and Y. B. Li, *J Food Protect* **68** (9), 1804-1811 (2005).
7. S. Shan, Z. Q. Zhong, W. H. Lai, Y. H. Xiong, X. Cui and D. F. Liu, *Food Control* **45**, 138-142 (2014).
8. X. A. Guan, H. J. Zhang, Y. N. Bi, L. Zhang and D. L. Hao, *Biomed Microdevices* **12** (4), 683-691 (2010).
9. S. Sengupta, J. E. Gordon and H. C. Chang, in *Microfluidics for Biological Applications*, edited by W. C. Tian and E. Finehout (Springer, 2009).
10. X. Li, E. Ximenes, M. A. R. Amalaradjou, H. B. Vibbert, K. Foster, J. Jones, X. Y. Liu, A. K. Bhunia and M. R. Ladisch, *Appl Environ Microb* **79** (22), 7048-7054 (2013).
11. G. Jenikova, J. Pazlarova and K. Demnerova, *Int Microbiol* **3** (4), 225-229 (2000).
12. H. Tsutsui and C. M. Ho, *Mech Res Commun* **36** (1), 92-103 (2009).

13. J. D. Adams, C. L. Ebbesen, R. Barnkob, A. H. J. Yang, H. T. Soh and H. Bruus, *J Micromech Microeng* **22** (7) (2012).
14. P. Augustsson and T. Laurell, *Lab Chip* **12** (10), 1742-1752 (2012).
15. L. C. Jellema, T. Mey, S. Koster and E. Verpoorte, *Lab Chip* **9** (13), 1914-1925 (2009).
16. H. C. Cui, Z. Huang, P. Dutta and C. F. Ivory, *Anal Chem* **79** (4), 1456-1465 (2007).
17. J. Voldman, *Annu Rev Biomed Eng* **8**, 425-454 (2006).
18. D. Holmes, N. G. Green and H. Morgan, *Ieee Eng Med Biol* **22** (6), 85-90 (2003).
19. C. F. Gonzalez and V. T. Remcho, *J Chromatogr A* **1079** (1-2), 59-68 (2005).
20. N. Pamme, *Lab Chip* **6** (1), 24-38 (2006).
21. A. H. J. Yang and H. T. Soh, *Anal Chem* **84** (24), 10756-10762 (2012).
22. F. Petersson, A. Nilsson, C. Holm, H. Jonsson and T. Laurell, *Analyst* **129** (10), 938-943 (2004).
23. F. Petersson, L. Aberg, A. M. Sward-Nilsson and T. Laurell, *Anal Chem* **79** (14), 5117-5123 (2007).
24. M. Nordin and T. Laurell, *Lab Chip* **12** (22), 4610-4616 (2012).
25. A. Nilsson, F. Petersson, H. Jonsson and T. Laurell, *Lab Chip* **4** (2), 131-135 (2004).
26. A. Lenshof, M. Evander, T. Laurell and J. Nilsson, *Lab Chip* **12** (4), 684-695 (2012).
27. T. Laurell, F. Petersson and A. Nilsson, *Chem Soc Rev* **36** (3), 492-506 (2007).
28. M. Koklu, A. C. Sabuncu and A. Beskok, *J Colloid Interf Sci* **351** (2), 407-414 (2010).
29. C. Grenvall, J. R. Folkenberg, P. Augustsson and T. Laurell, *Cytom Part A* **81A** (12), 1076-1083 (2012).
30. C. Grenvall, P. Augustsson, J. R. Folkenberg and T. Laurell, *Anal Chem* **81** (15), 6195-6200 (2009).
31. I. Gonzalez, L. J. Fernandez, T. E. Gomez, J. Berganzo, J. L. Soto and A. Carrato, *Sensor Actuat B-Chem* **144** (1), 310-317 (2010).
32. M. Evander, L. Johansson, T. Lilliehorn, J. Piskur, M. Lindvall, S. Johansson, M. Almqvist, T. Laurell and J. Nilsson, *Anal Chem* **79** (7), 2984-2991 (2007).
33. M. A. Burguillos, C. Magnusson, M. Nordin, A. Lenshof, P. Augustsson, M. J. Hansson, E. Elmer, H. Lilja, P. Brundin, T. Laurell and T. Deierborg, *Plos One* **8** (5) (2013).
34. M. Wiklund, R. Green and M. Ohlin, *Lab Chip* **12** (14), 2438-2451 (2012).
35. P. B. Muller, R. Barnkob, M. J. H. Jensen and H. Bruus, *Lab Chip* **12** (22), 4617-4627 (2012).
36. C. Schrader, A. Schielke, L. Ellerbroek and R. John, *Journal of Applied Microbiology* **113**, 1014-1026 (2012).
37. D. A. Buzatu, T. J. Moskal, A. J. Williams, W. Mae Cooper, W. B. Mattes and J. G. Wilkes, *Plos One* **9** (e94254), 1-10 (2014).
38. P. F. G. Wolffs, K. Glencross, R. Thibaudau and M. W. Griffiths, *Appl Environ Microb* **72** (6), 3896-3900 (2006).
39. T. McCreedy, *Anal Chim Acta* **427** (1), 39-43 (2001).
40. ISO, in *International standard*, edited by ISO (2007), pp. 7218.
41. P. A. G. D.A. Boehma, and S.Z. Huaa, *Sensors and Actuators B* **126**, 508-524 (2007).
42. H. Jonsson, C. Holm, A. Nilsson, F. Petersson, P. Johnsson and T. Laurell, *Ann Thorac Surg* **78** (5), 1572-1578 (2004).
43. H. W. Hou, A. A. S. Bhagat, W. C. Lee, S. Huang, J. Han and C. T. Lim, *Micromachines-Basel* **2** (3), 319-343 (2011).
44. M. L. Chiu, W. Lawi, S. T. Snyder, P. K. Wong, J. C. Liao and V. Gau, *Jala-J Lab Autom* **15** (3), 233-242 (2010).

45. P. D. Ohlsson, K. Petersson, P. Augustsson and T. Laurell, presented at the 17th International Conference on Miniaturized Systems for Chemistry and Life Sciences, Freiburg, Germany, 2013 (unpublished).
46. J. D. Esko and N. Sharon, in *Essentials of Glycobiology* (Cold Spring Harbor 2009).
47. N. Sharon and I. Ofek, *Glycoconjugate J* **17** (7-9), 659-664 (2000).
48. V. Schönenbrücher, E. T. Mallinson and M. Bülte, *Int J Food Microbiol* **123**, 61-66 (2008).